Electronic Supplementary Material (ESI) for ChemComm.

Supporting Information for

Electrocatalytic reduction of CO_2 in water by a *C*-functionalized Ni-cyclam complex grafted onto carbon

Amélie Forget,[a] Matthieu Regnacq,[a] Christophe Orain,[a] Ewen Touzé,[a] Evan Lelong,[a] Christophe Brandily,[b] Hélène Bernard,[a] Raphaël Tripier,*[a] Nicolas Le Poul*[a]

Table of contents

1. Materials and Methods

General. $NaNO_2$ was purchased from Sigma-Aldrich; KCl was obtained from Acros. $NaHCO_3$ and $LiClO_4$ (electrochemical grade) were purchased from Sigma-Aldrich. Diluted HCl solutions (0.5 M) were prepared from concentrated HCl (32%) purchased from Merck. Cyclam (Ligand **L2**) was purchased from Chematech. N1,N8-dibenzyl-p-NO_2-Bn-cyclam[1,2] and cyclamPO[3] were synthesized according to reported procedures. Acetonitrile (ACN) was freshly distilled over CaH_2 under N_2. MilliQ water (resistivity of 18.2 MΩ.cm, Total Organic Carbon TOC < 10 ppb) was used for all experiments. The supporting electrolyte NBu_4PF_6 was synthesized from NBu_4OH (Fluka) and HPF_6 (Aldrich). It was then purified, dried under vacuum for 48 hours at 100° C, then kept under N_2 in the glovebox before use. Commercial-grade thin Multi-Walled Carbon Nanotubes (MWCNTs) (9.5 nm diameter, 1.5 µm long, purity > 90%, Nanocyl) were generously provided by Dr N. Lalaoui and Dr. F. Giroud. They were used as received.

Methods. NMR spectra were recorded in $CDCl_3$, CD_3CN at ambient temperature on a Bruker AC 300 spectrometer. For high-resolution mass spectrometry, a HRMS Q-Tof MaXis instrument was used, with sources ESI, APCI, APPI, nano-ESI (at the Institute of Organic and Analytic Chemistry, ICOA).UV-Visible spectra were obtained an Agilent Cary 500 spectrometer. Electrochemical studies of the complexes **1**-**3** in CH_3CN/H_2O (4:1) / NBu_4PF_6 0.1 M, $H_2O/NaHCO_3$ 0.2 M or $H_2O/LiClO_4$ 0.1 M were performed under inert atmosphere (argon) with a home-designed 3-electrodes cell displaying separated compartments for the reference and auxiliary electrodes (WE: glassy carbon, gold RE: Ag/AgCl/NaCl 3M, CE: graphite rod). The potential of the cell was controlled by an AUTOLAB PGSTAT 302 (Metrohm) potentiostat monitored by the NOVA software. All electrodes were polished on an alumina slurry (1 µm) and sonicated in water then acetone during 5 minutes each, then dried with N_2 flow. Au surfaces were activated by cycling 40 times between 0.4 and 1.6 V vs Ag/AgCl at 0.2 $V.s^{-1}$ in diluted sulfuric acid (0.5 M). XPS measurements were carried out with K-Alpha+ apparatus (ThermoFisher Scientific) at the ITODYS (Paris). Controlled-potential electrolyses (CPE) were performed with a specifically designed electrochemical air-tight cell (RE: Ag/AgCl/NaCl 3M, CE: graphite rod, WE: Glassy Carbon (0.07 cm^2) functionalized MWCNTs and complex **1**) under stirring. The electrolytic solution ($NaHCO_3$ 0.2 M/H_2O) was saturated with CO_2 before the electrolysis (pH = 6.8). The gas mixture was extracted with a 5 mL gas-tight Hamilton® syringe after 1 h30, and injected into the gas chromatography apparatus. Gas chromatography measurements were carried out with a Shimadzu Nexis GC-2030 apparatus equipped with PoraPLOT Q (PPQ) and MolSieve 5A (MS5A) column channels and a BID detector. Calibrations were performed by using gas mixtures of CH_4, CO_2 and CH4, CO and H_2 of known concentration (purchased from Air Liquide). Centrifugation was carried out with a Jouan B4i apparatus.

Diazonium grafting method. The arylamine compound and $NaNO_2$ (1:1) were introduced in HCl 0.5 M and degassed under argon at room temperature. After 15 minutes, the electrodeposition was operated by applying a specific reduction potential during 100 s. After grafting, all electrodes were sonicated 5 minutes in water and 5 minutes in ethanol, then dried with argon.

Pre-modication of GC electrodes with carbon nanotubes. Films of MWCNTs were obtained by deposition of 20 µL of a solution 3 mg mL^{-1} of MWCNTs in N-Methyl-2-Pyrrolidone (NMP) onto a glassy carbon surface (0.07 cm^2). The solvent was then evaporated under vacuum for 24 h. The resulting electrodes were then rinsed with $EtOH/H_2O$ then H_2O before diazonium grafting.

2. Syntheses of ligands and Ni^{II} complexes

2.1 Synthesis of ligand L1

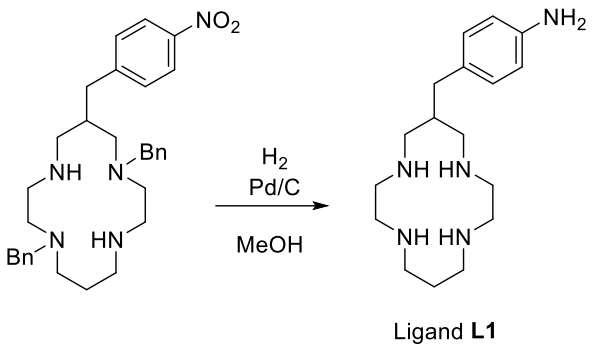

Scheme S1. Synthesis of the p-H_2N-Bn-cyclam ligand (**L1**) from N1,N8-dibenzyl-*p*-NO_2-Bn-cyclam.[1, 2]

N1,N8-dibenzyl-*p*-NO_2-Bn-cyclam1,2 (300 mg; 0.58 mmol) was dissolved in 20mL of methanol. Pd/C (10% w; 200 mg; 0.2 mmol; 0.3 eq.) was added and the mixture was stirred under H_2 atmosphere for one week. The palladium was filtered out on celite and the filtrate was evaporated. The titled compound was obtained as a beige oil (130 mg; 0.42 mmol). Yield: 73%. ^{1}H NMR (500MHz, D_2O, 298K) δ (ppm): 7.02-7.00 (m, 2H), 6.74-6.71 (m, 2H), 2.69-2.53 (m, 14H) 2.47-2.42 (m, 4H), 1.92-1.91 (m, 1H), 1.65-1.60 (m, 2H); ^{13}C Jmod NMR (125MHz, D_2O, 298K) δ (ppm): 144.1, 131.3, 129.9, 116.4, 52.0, 46.9, 46.6, 46.4, 38.8, 36.6, 26.6.

2.2 Synthesis of ligand L3

Ligand **L3** was synthesized starting from cyclamPO.[3]

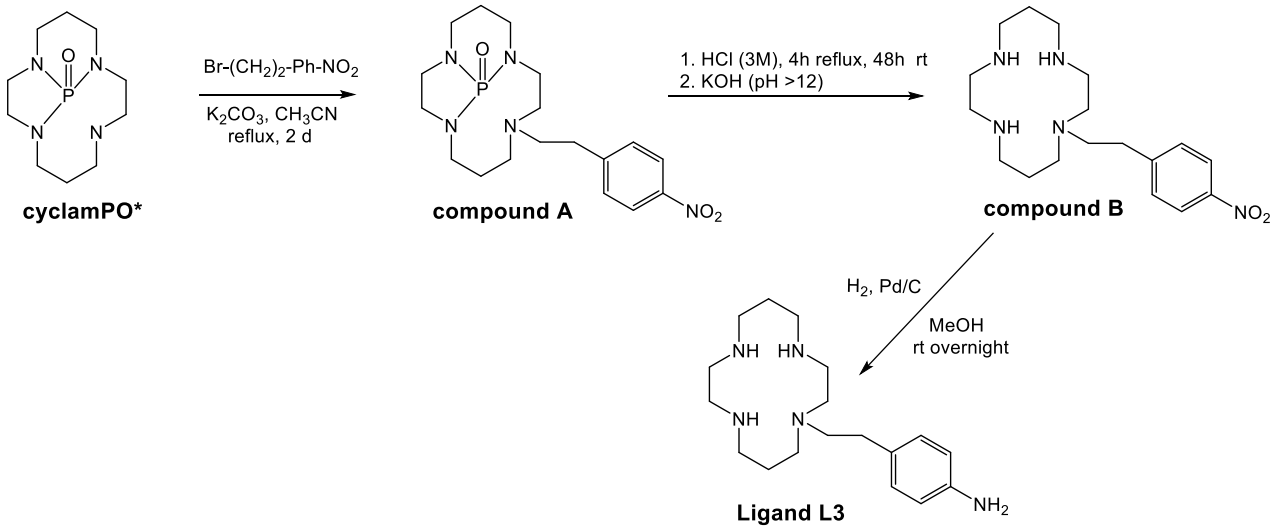

Scheme S2. Synthesis of *N*-(*p*-H_2N-Ph-$(CH_2)_2$)-cyclam ligand (**L3**).

Synthesis of compound A:

4-nitrophenethyl bromide (460 mg, 2 mmol, 2 eq.) was added on a solution of cyclam-PO[3] (244 mg, 1 mmol, 1 eq.) in CH_3CN (15 mL) in presence of K_2CO_3 (414 mg, 3mmol) and stirred 2 d at reflux. The mixture was filtered and the filtrate was evaporated under reduced pressure. The residue was then purified by chromatography on silica gel with CH_2Cl_2/MeOH gradient. Compound A was obtained as beige powder (300 mg, yield = 76 %) and used in next step without more purification. ^{1}H NMR (400 MHz, $CDCl_3$, 298 K) δ (ppm): 8.13-8.11 (m, 2H), 7.36-7.34 (m, 2H), 3.72-3.51 (m, 2H), 3.35-3.22 (m, 3H), 3.14-2.79 (m, 8H), 2.75-2.60 (m, 3H), 2.53-2.43 (m, 4H), 1.92-1.73 (m, 2H), 1.47-1.43 (m, 2H). ^{13}C Jmod NMR (75 MHz, $CDCl_3$, 298 K) δ (ppm): [148.6, 146.3] (C_{Ar}), [129.6, 123.5] (CH_{Ar}), [54.7, 53.4, 51.9, 51.6, 45.6 (d, J = 15.5 Hz), 44.2 (d, J = 11.3 Hz), 42.0, 41.6, 40.6 (d, J = 2.9 Hz)] (CH_2-α-N), 33.8 (CH_2-α-$PhNO_2$), [26.0, 22.0] (CH_2-β-N). ^{31}P NMR (160 MHz, $CDCl_3$, 298 K) δ (ppm): 26.2.

Synthesis of the compound B: 1-(4-nitrophenethyl)-1,4,8,11-tetraazacyclotetradecane:

Compound A (300 mg, 0.76 mmol) was dissolved in HCl 3 M (10 mL) and stirred 4 h at reflux then 48 h at rt. At 0°C, KOH pellets was added until pH reached 12 then aqueous layer was extracted with $CHCl_3$ (3 x 40 mL). Organic layers were combined, dried with $MgSO_4$, filtered and dried under reduced pressure. Compound B was obtained as brown oil (193 mg, yield = 72 %) and used in next step without more purification.^{13}C Jmod NMR (75 MHz, $CDCl_3$, 298 K) δ (ppm): [148.6, 146.1] (C_{Ar}), [129.5, 123.3] (CH_{Ar}), [54.4, 53.6, 52.6, 50.8, 49.1, 48.9, 48.4, 47.7, 47.3] (CH_2-α-N), 31.6 (CH_2-α-$PhNO_2$), [28.5, 25.9] (CH_2-β-N).

Synthesis of *N*-(*p*-H_2N-Ph-$(CH_2)_2$)-cyclam (**L3**):

4-(2-(1,4,8,11-tetraazacyclotetradecan-1-yl)ethyl)aniline:
Pd/C (10 w%, 220 mg, 0.2 mmol, 0.36 eq) was added to a solution of compound B (193 mg, 0.55 mmol) in MeOH (20 mL) and stirred under H_2 atmosphere at rt overnight. The mixture was filtered on celite and solvent removed under reduced pressure. Ligand **L3** was obtained as a yellow oil (175 mg, quantitative yield). ^{1}HNMR (400 MHz, $CDCl_3$, 298 K) δ (ppm): 7.00-6.97 (m, 2H), 6.61-6.58 (m, 2H), 3.79 (bs, 5H, NH), 2.85-2.41 (m, 20H), 1.80-1.70 (m, 4H). ^{13}C Jmod NMR (75 MHz, $CDCl_3$, 298 K) δ (ppm): [144.5, 130.1] (C_{Ar}), [129.5, 115.1] (CH_{Ar}), [54.4, 53.0, 53.0, 50.5, 49.1, 48.6, 48.1, 47.0, 46.9] (CH_2-α-N), 30.9 (CH_2-α-$PhNO_2$), [27.0, 25.5] (CH_2-β-N).

2.3 Syntheses of complexes 1-3

[Ni^{II}(*p*- H_2N-Bn-cyclam)]Cl_2 (complex **1**), [Ni^{II}(cyclam)]Cl_2 (complex **2**) and [Ni^{II} *N*-(*p*-H_2N-Ph-$(CH_2)_2$)-cyclam]Cl_2 (complex **3**). The syntheses of complexes **1**-**3** were adapted from reported procedure:[4] the macrocyclic ligand (0.33 mmol) was solubilized in water (10 mL) and 6 equivalents of $NaHCO_3$ (2 mmol) were added, under magnetic stirring. Gas formation was observed and after 30 minutes, 1.2 equivalent of $NiCl_2$ (0.40 mmol) was added to the mixture, followed by addition of ethanol (3 mL). The mixture was stirred for two hours at 38°C. The solvents were then evaporated thanks to a rotary evaporator, and the resulting solid was dissolved in 20 mL of ethanol for purification. After centrifugation (4000 RPM) for 15 min, filtration, evaporation of ethanol and drying under vacuum during one night, a colored (beige-brown for **1**, purple for **2** and yellow-brown for **3**) nickel(II) dichloride complex was obtained in quantitative yield.

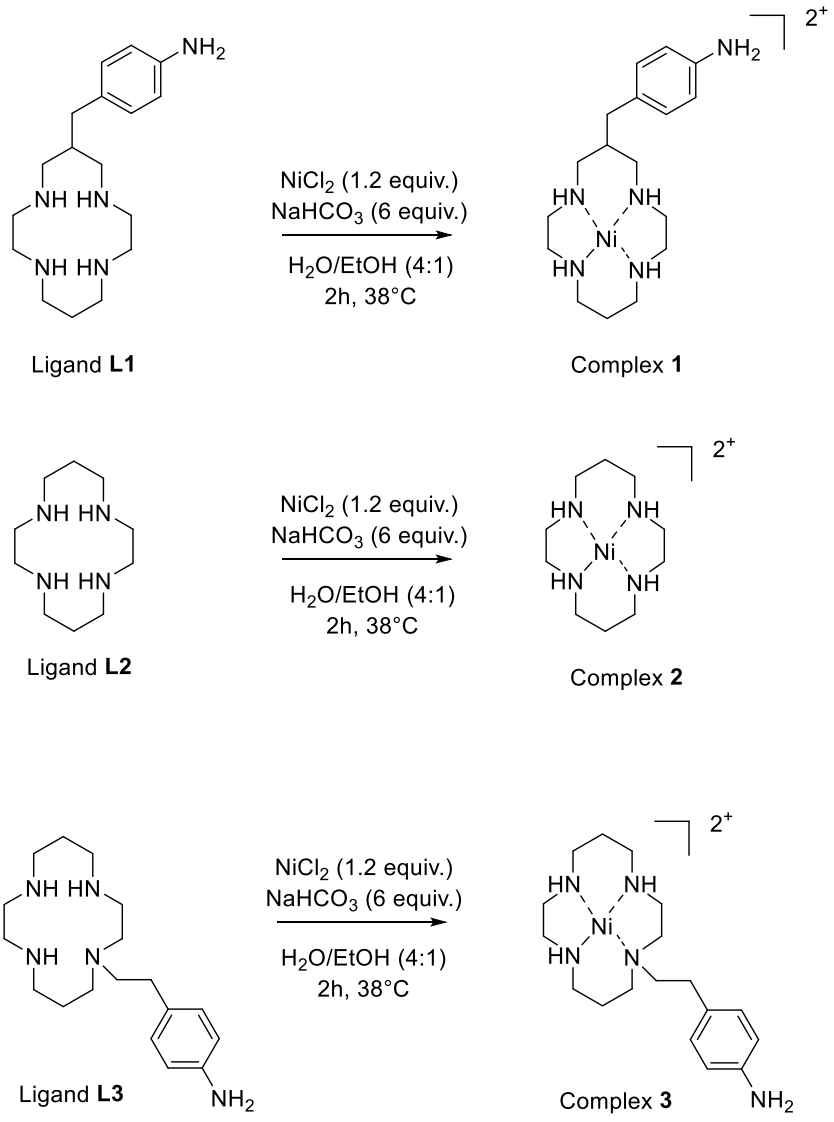

Scheme S3. Synthetic procedures for complexes **1**-**3**.

3. Spectroscopic characterization of ligands and complexes

3.1 ^{1}H and ^{13}C NMR characterization of ligand L1

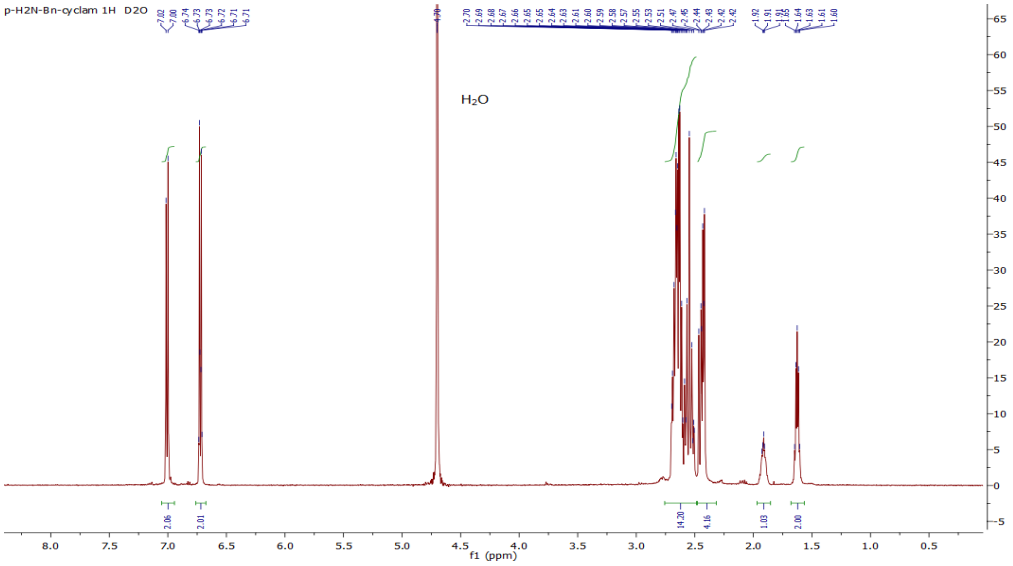

Figure S1. ^{1}H NMR spectrum (500MHz, D_2O, 298K) of ligand **L1**.

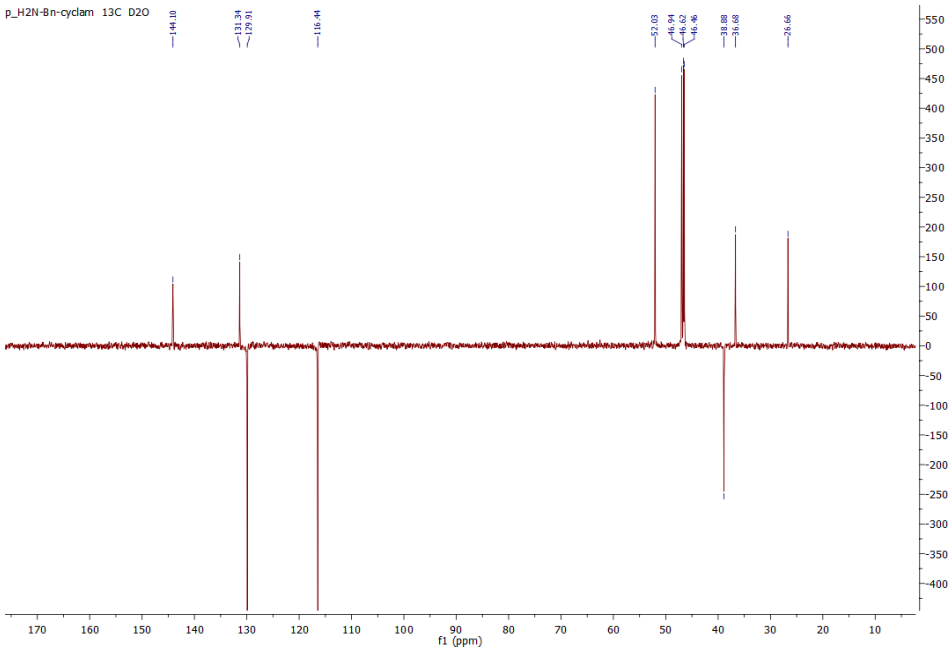

Figure S2. ^{13}C NMR spectrum (125MHz, D_2O, 298K) of ligand **L1**.

3.2 ^{1}H and ^{13}C NMR characterization of Ligand L3, compounds A and B.

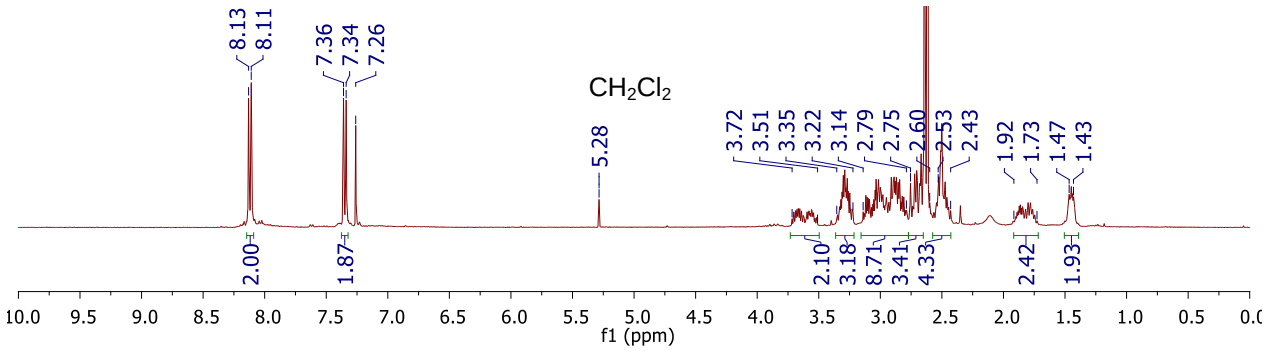

Figure S3. ^{1}H NMR (400 MHz, $CDCl_3$, 298 K) spectrum of compound A.

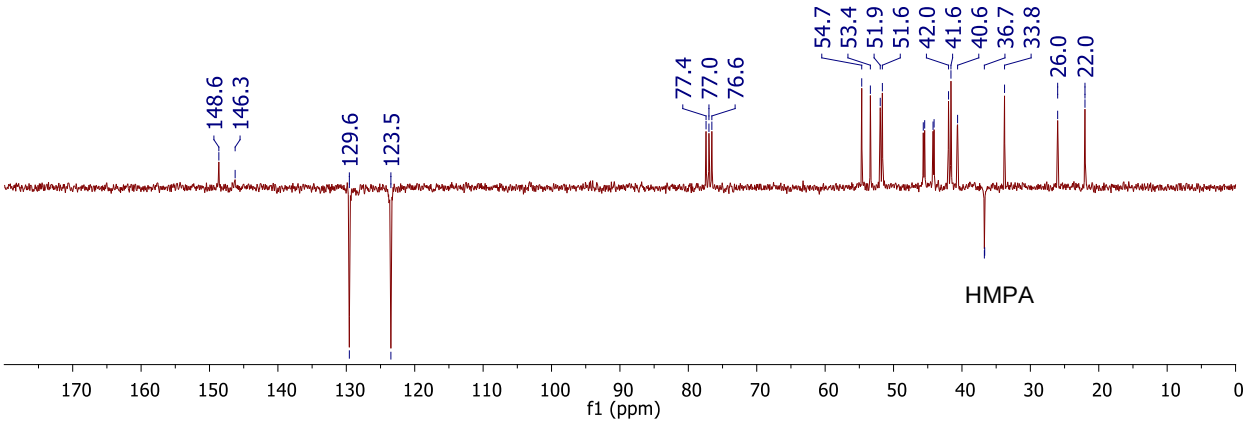

Figure S4. ^{13}C Jmod NMR (75 MHz, $CDCl_3$, 298 K) spectrum of compound A.

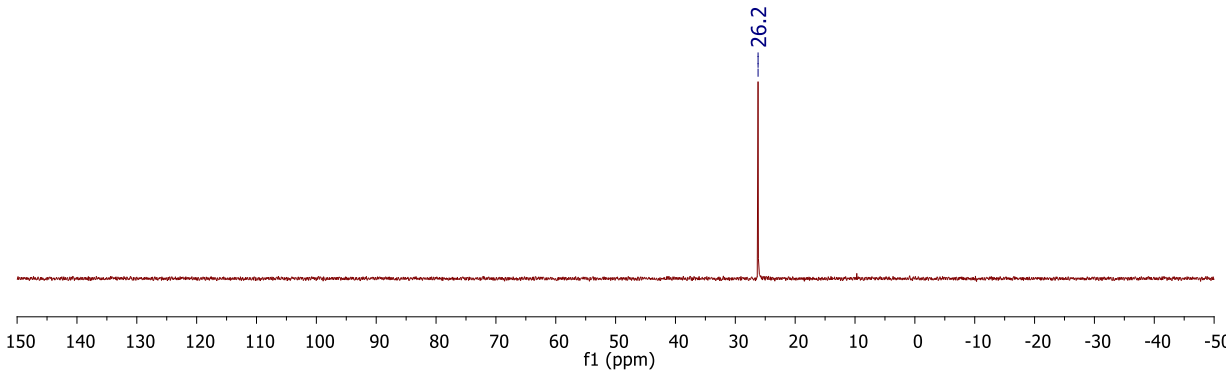

Figure S5. ^{31}P NMR (160 MHz, $CDCl_3$, 298 K) spectrum of compound A.

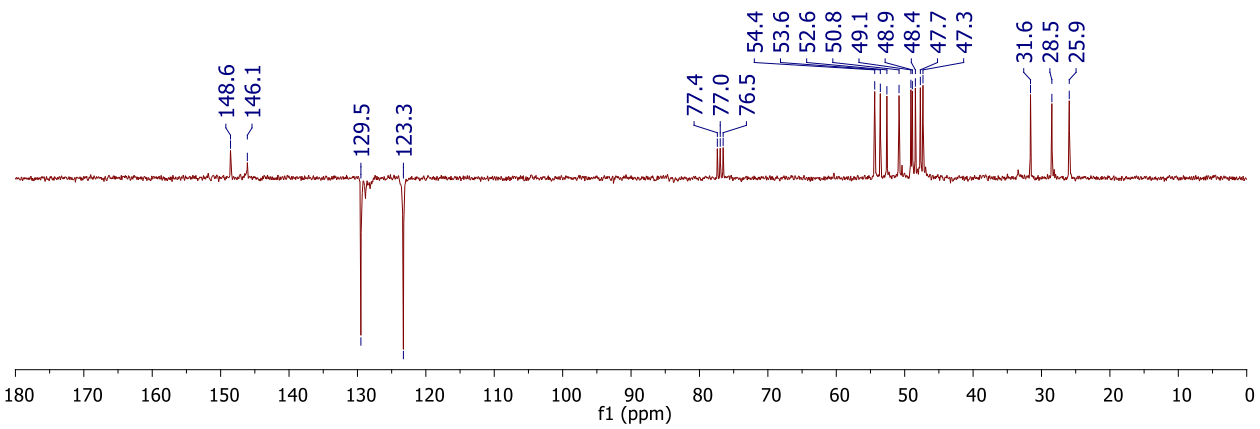

Figure S6. ^{13}C Jmod NMR (75 MHz, $CDCl_3$, 298 K) spectrum of compound B.

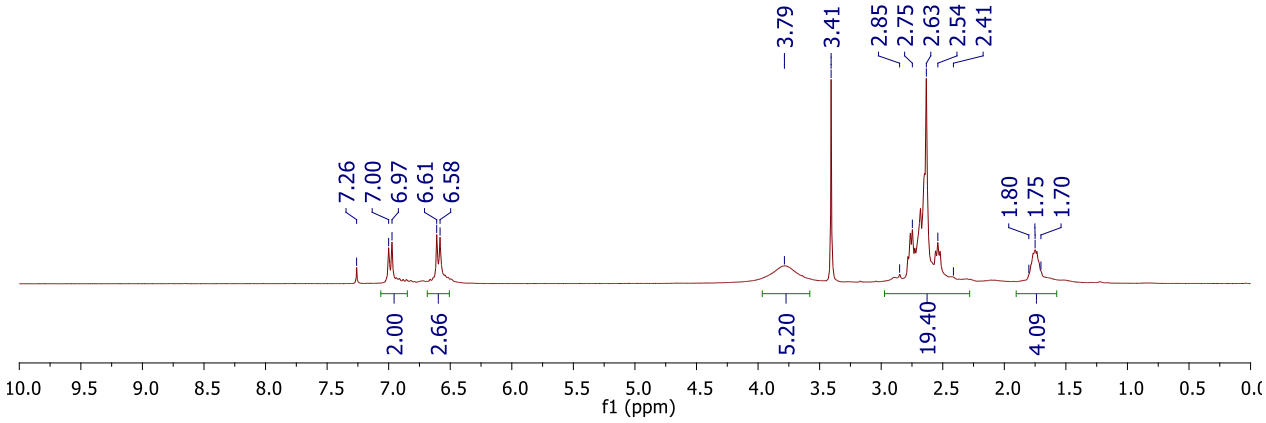

Figure S7. ^{1}H NMR (400 MHz, $CDCl_3$, 298 K) spectrum of ligand **L3**.

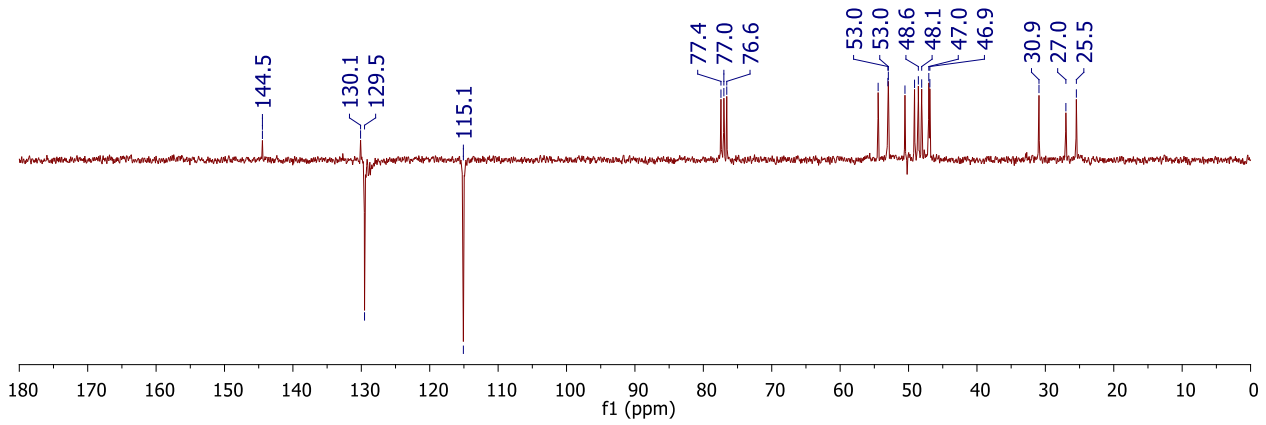

Figure S8.^{13}C Jmod NMR (75 MHz, $CDCl_3$, 298 K) spectrum of ligand **L3.**

3.3. Mass spectrometry characterization of ligands and complexes

Ligand **L1**

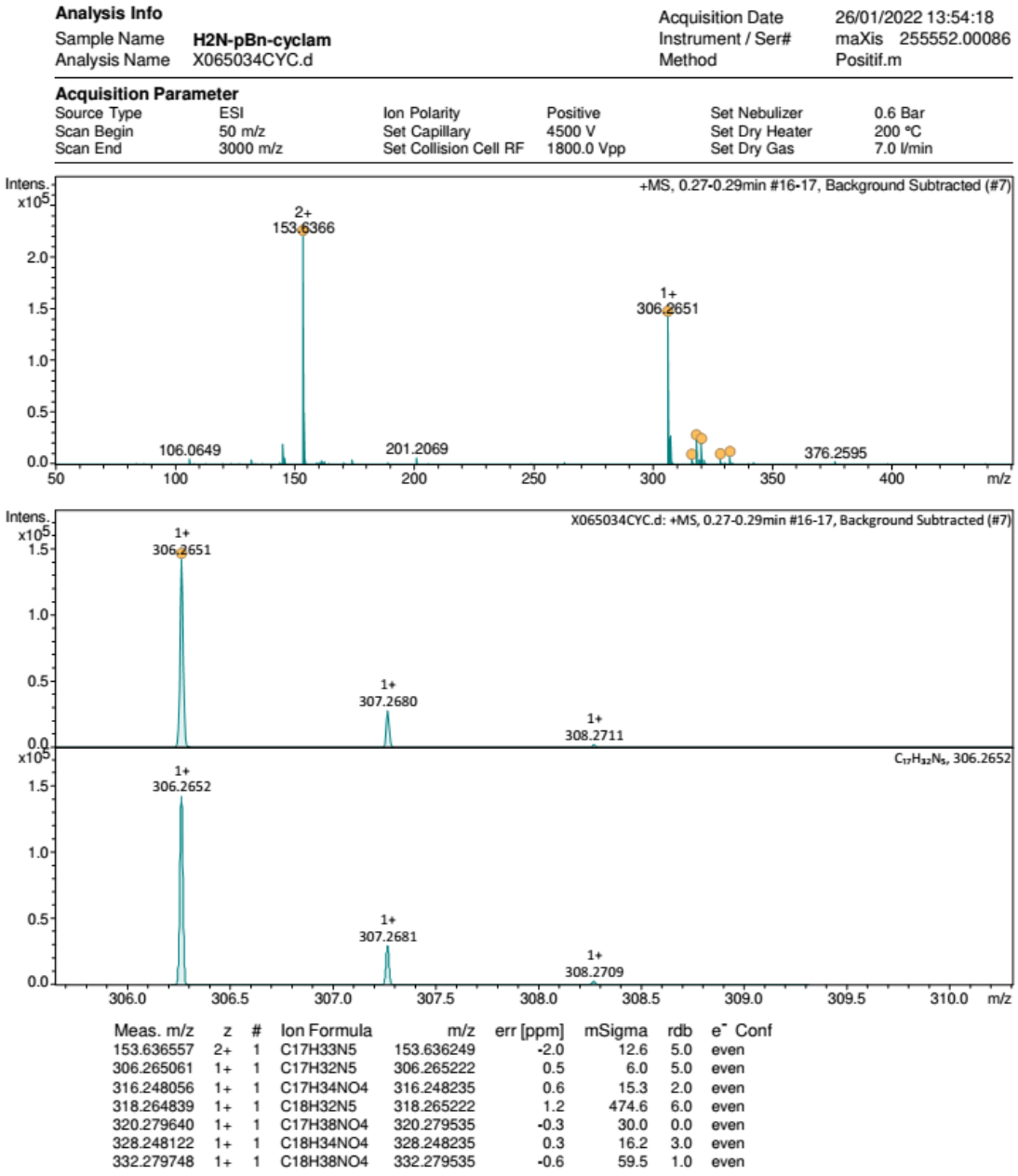

Meas. m/z	z	#	Ion Formula	m/z	err [ppm]	mSigma	rdb	e⁻ Conf
153.636557	2+	1	C17H33N5	153.636249	-2.0	12.6	5.0	even
306.265061	1+	1	C17H32N5	306.265222	0.5	6.0	5.0	even
316.248056	1+	1	C17H34NO4	316.248235	0.6	15.3	2.0	even
318.264839	1+	1	C18H32N5	318.265222	1.2	474.6	6.0	even
320.279640	1+	1	C17H38NO4	320.279535	-0.3	30.0	0.0	even
328.248122	1+	1	C18H34NO4	328.248235	0.3	16.2	3.0	even
332.279748	1+	1	C18H38NO4	332.279535	-0.6	59.5	1.0	even

Figure S9. High-Resolution Mass spectrum of ligand **L1**.

Ligand **L3**

Analysis Info

Sample Name	**H2N-pBn-(CH2)2-N-cyclam**	Acquisition Date	26/01/2022 13:52:52
Analysis Name	X065033CYC.d	Instrument / Ser#	maXis 255552.00086
		Method	Positif.m

Acquisition Parameter

Source Type	ESI	Ion Polarity	Positive	Set Nebulizer	0.6 Bar
Scan Begin	50 m/z	Set Capillary	4500 V	Set Dry Heater	200 °C
Scan End	3000 m/z	Set Collision Cell RF	1800.0 Vpp	Set Dry Gas	7.0 l/min

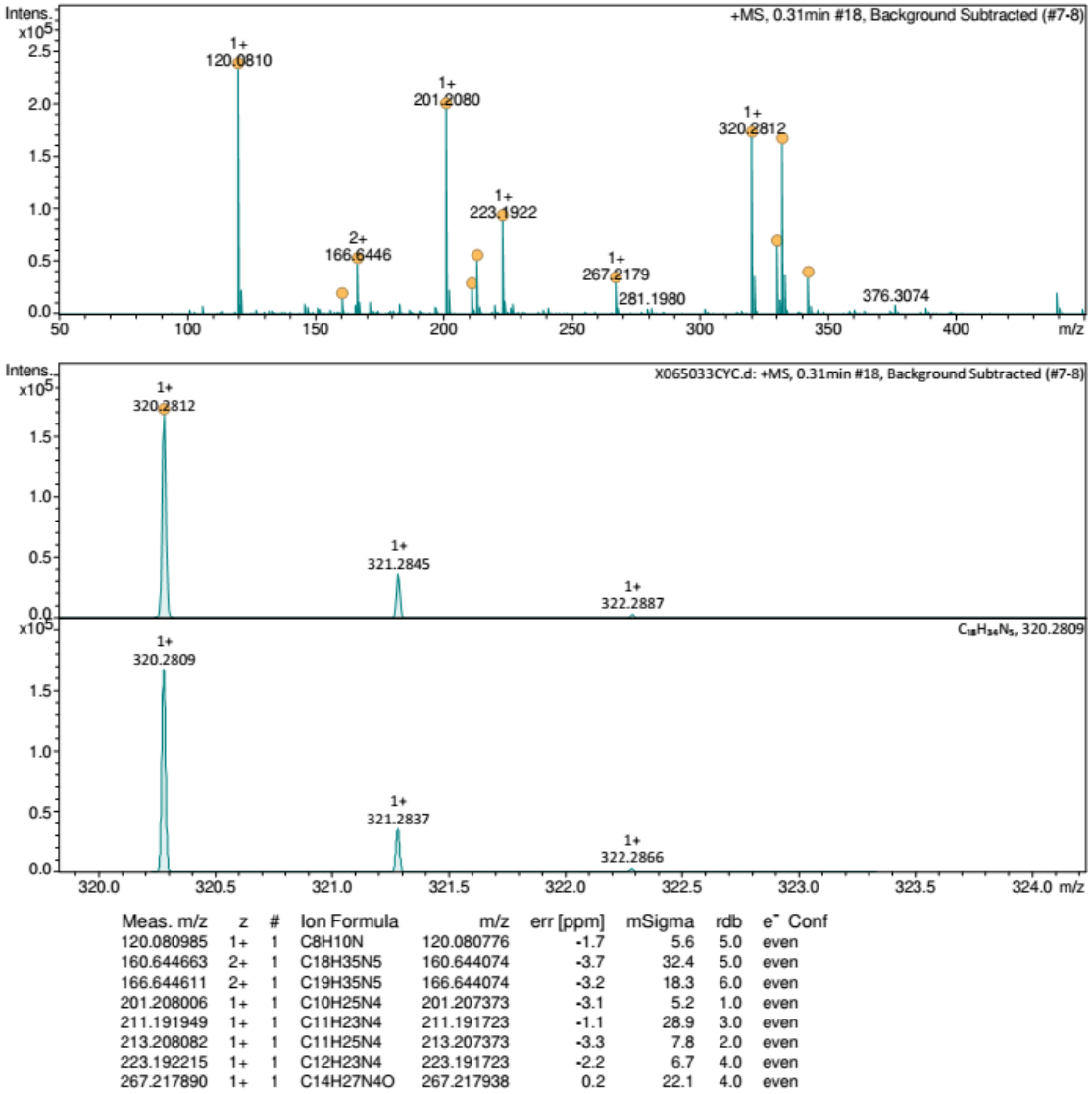

Meas. m/z	z	#	Ion Formula	m/z	err [ppm]	mSigma	rdb	e⁻ Conf
120.080985	1+	1	C8H10N	120.080776	-1.7	5.6	5.0	even
160.644663	2+	1	C18H35N5	160.644074	-3.7	32.4	5.0	even
166.644611	2+	1	C19H35N5	166.644074	-3.2	18.3	6.0	even
201.208006	1+	1	C10H25N4	201.207373	-3.1	5.2	1.0	even
211.191949	1+	1	C11H23N4	211.191723	-1.1	28.9	3.0	even
213.208082	1+	1	C11H25N4	213.207373	-3.3	7.8	2.0	even
223.192215	1+	1	C12H23N4	223.191723	-2.2	6.7	4.0	even
267.217890	1+	1	C14H27N4O	267.217938	0.2	22.1	4.0	even

Figure S10. High-Resolution Mass spectrum of ligand.

Complex **1**

Chemical Formula: $C_{17}H_{31}N_5Ni$, corresponding to $[M]^{2+}$ where M=Ni(*p*-H_2N-Bn-cyclam)
Exact Mass: m/z = 181.5961; Found: m/z = 181.5958
Detection of traces: m/z = 398.1611 for $[M+Cl]^+$; m/z = 362.1843 for $[M-H]^+$

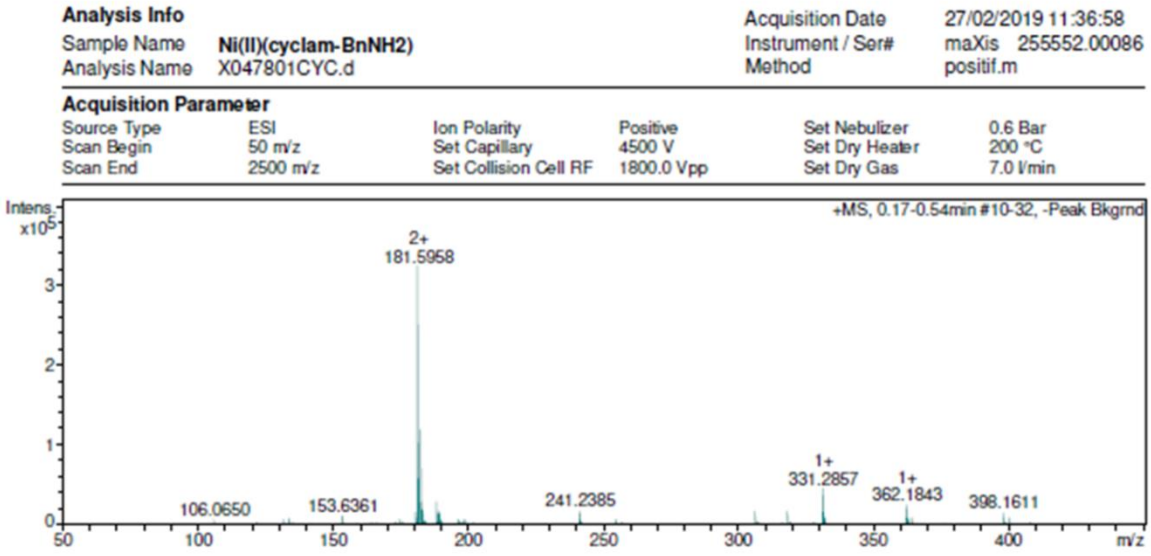

Figure S11. High-Resolution Mass spectrum of complex **1**.

Complex **2**

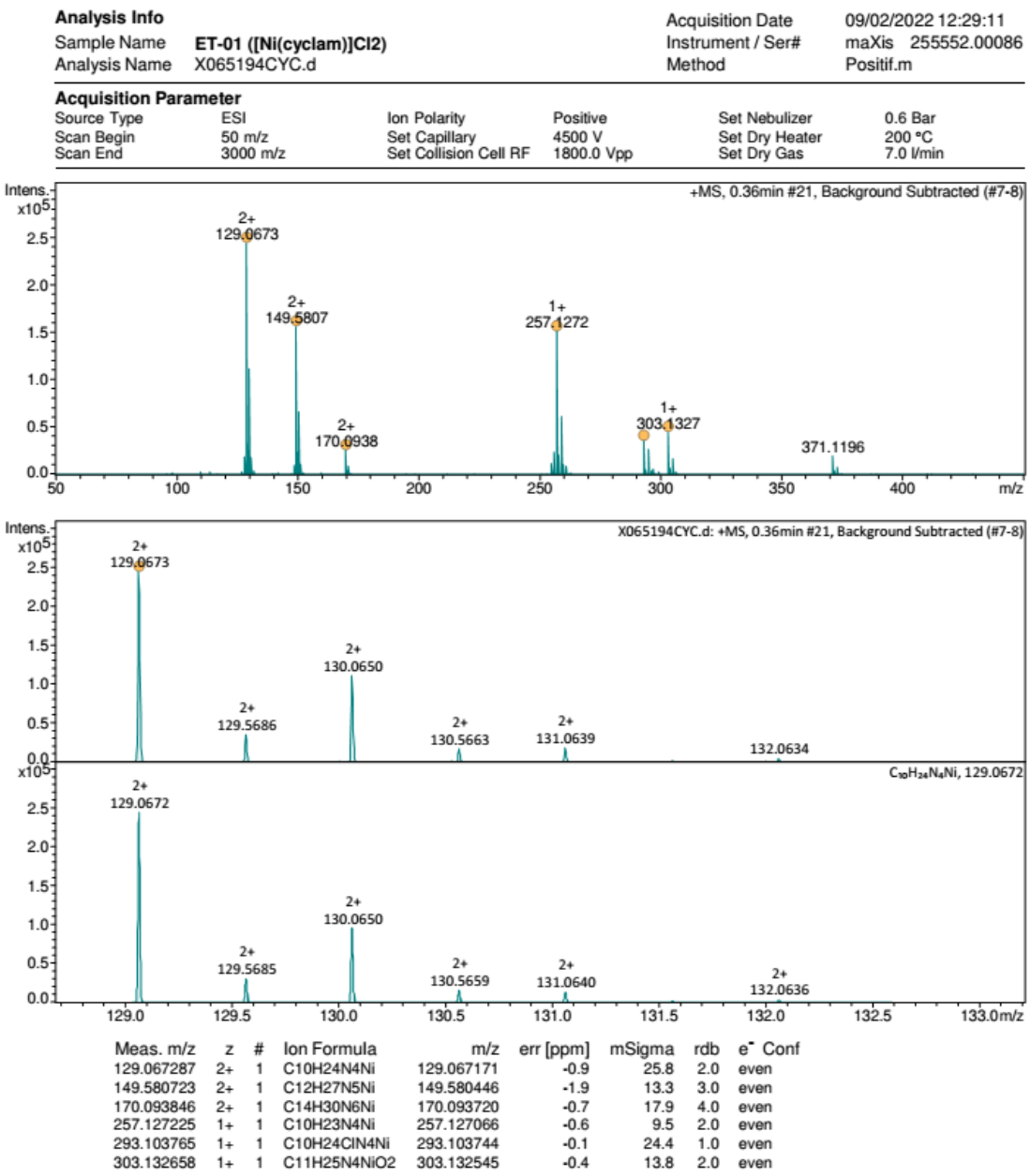

Meas. m/z	z	#	Ion Formula	m/z	err [ppm]	mSigma	rdb	e⁻ Conf
129.067287	2+	1	C10H24N4Ni	129.067171	-0.9	25.8	2.0	even
149.580723	2+	1	C12H27N5Ni	149.580446	-1.9	13.3	3.0	even
170.093846	2+	1	C14H30N6Ni	170.093720	-0.7	17.9	4.0	even
257.127225	1+	1	C10H23N4Ni	257.127066	-0.6	9.5	2.0	even
293.103765	1+	1	C10H24ClN4Ni	293.103744	-0.1	24.4	1.0	even
303.132658	1+	1	C11H25N4NiO2	303.132545	-0.4	13.8	2.0	even

Figure S12. High-Resolution Mass spectrum of complex **2**.

Complex **3**

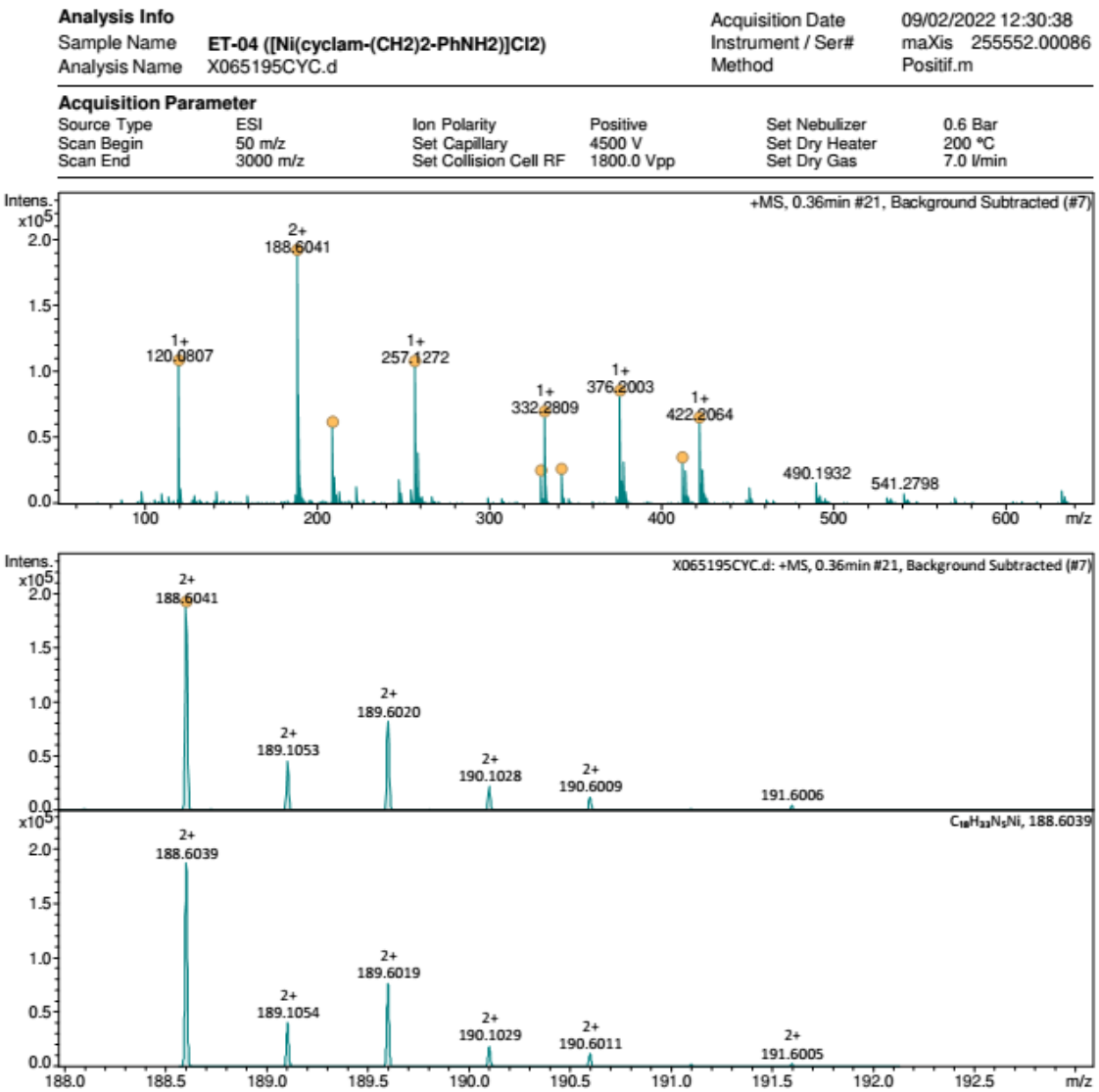

Meas. m/z	z	#	Ion Formula	m/z	err [ppm]	mSigma	rdb	e⁻ Conf
120.080724	1+	1	C8H10N	120.080776	0.4	12.5	5.0	even
188.604147	2+	1	C18H33N5Ni	188.603921	-1.2	17.9	6.0	even
209.117371	2+	1	C20H36N6Ni	209.117195	-0.8	22.9	7.0	even
257.127181	1+	1	C10H23N4Ni	257.127066	-0.4	9.9	2.0	even
330.265218	1+	1	C19H32N5	330.265222	0.0	693.6	7.0	even
332.280855	1+	1	C19H34N5	332.280873	0.1	4.0	6.0	even
342.265735	1+	1	C20H32N5	342.265222	-1.5	18.9	8.0	even
376.200251	1+	1	C18H32N5Ni	376.200565	0.8	10.8	6.0	even

Figure S13. High-Resolution Mass spectrum of complex **3**.

3.4. UV-Vis spectroscopy characterization of complexes 1-3

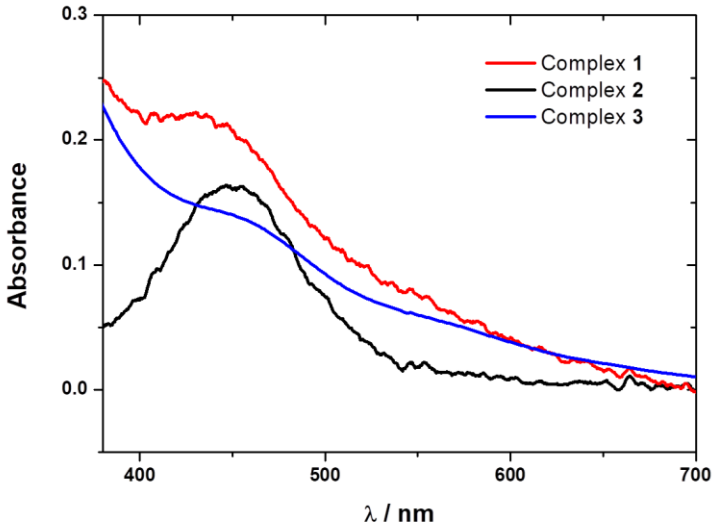

Figure S14. UV-Vis spectra (optical length: 10 mm) of complexes **1**-**3** (5 mM) in H_2O.

4. Voltammetric characterization of complexes 1-3

4.1. CV of complexes 1-3 in CH_3CN/H_2O (4:1) under Ar and CO_2

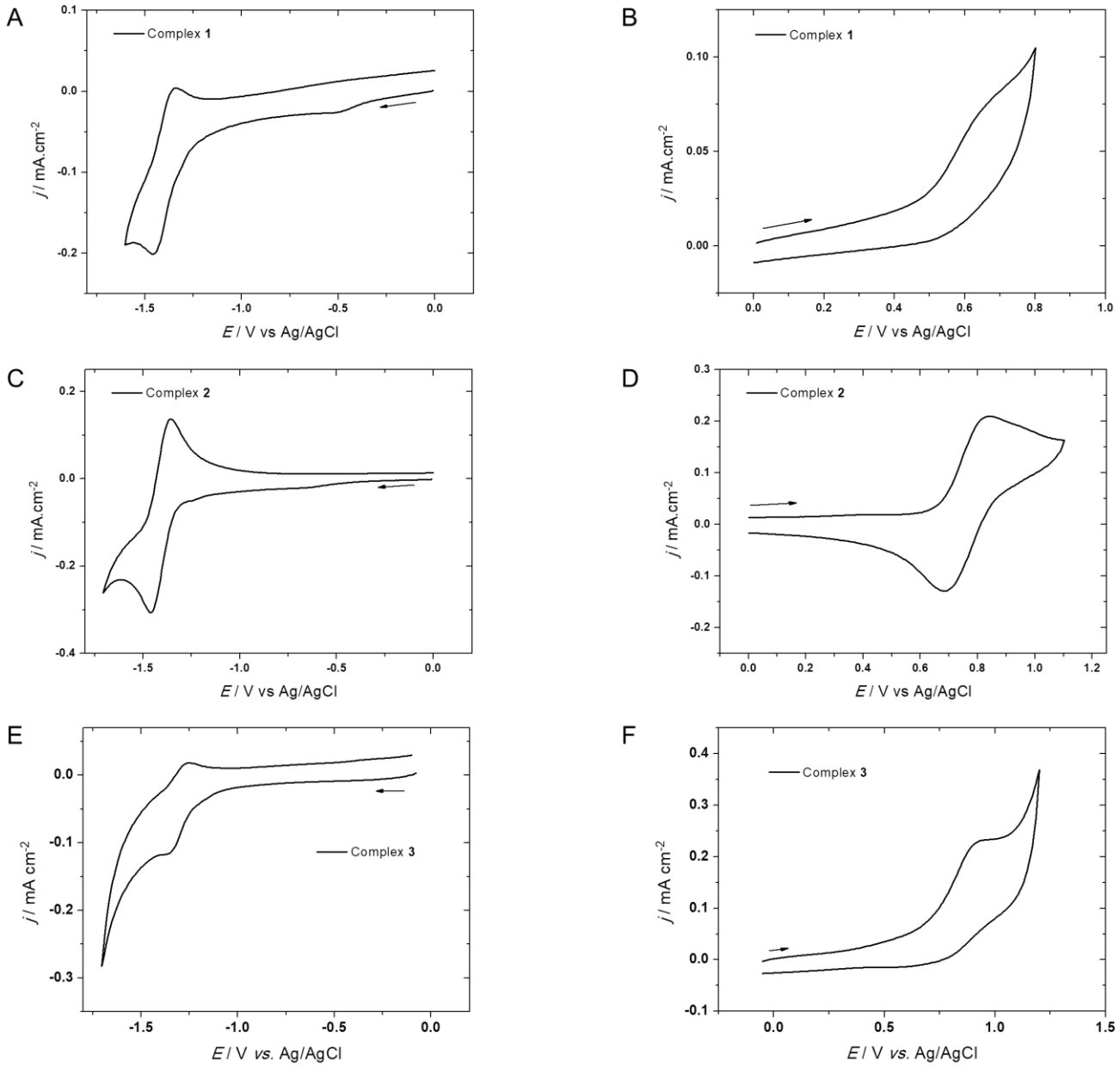

Figure S15. CVs (v = 0.1 $V.s^{-1}$) at a glassy carbon working electrode of A) and B) complex **1**, C) and D) complex **2** and E) and F) complex **3** in H_2O/CH_3CN (1:4) / NBu_4PF_6 0.1 M under argon: A, C, E) negative scanning direction; B, D, F) positive scanning direction. E / V *vs*. Ag/AgCl.

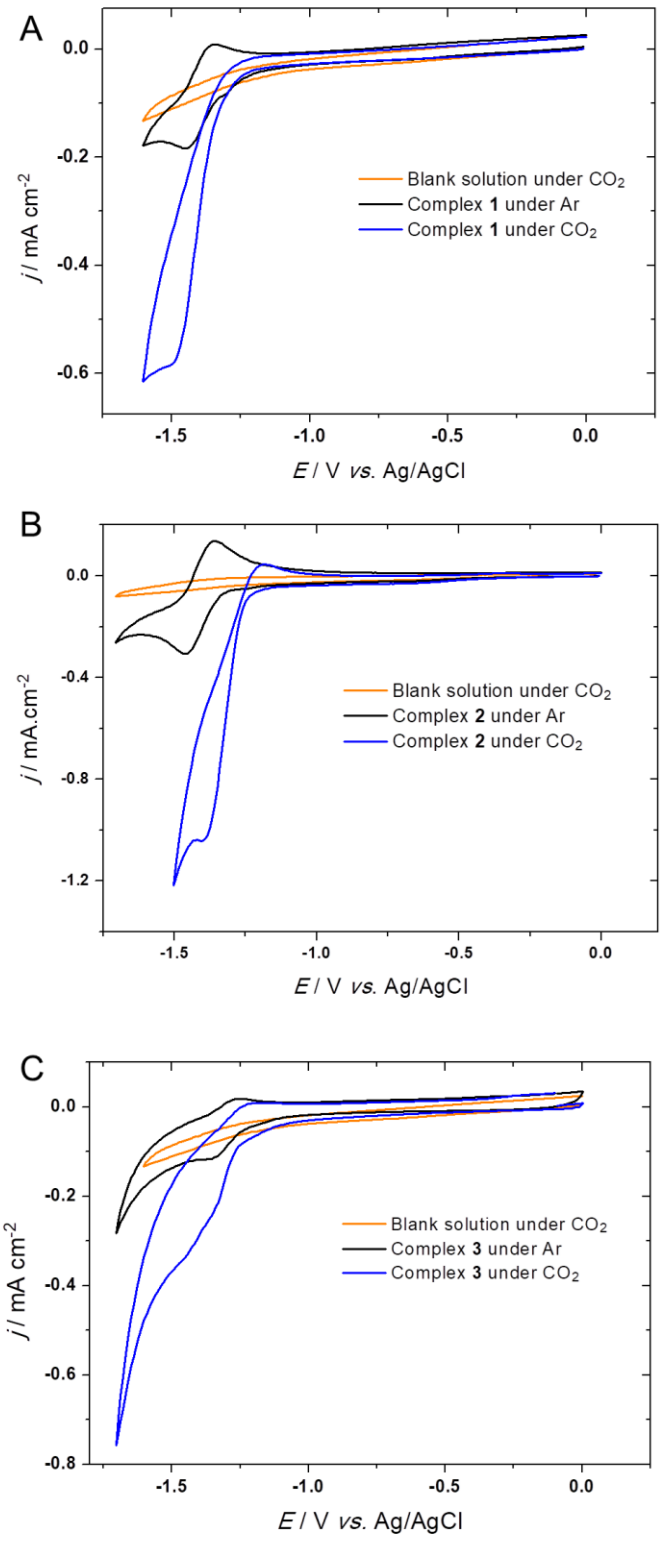

Figure S16. CVs (v = 0.1 V.s^{-1}) at a glassy carbon working electrode of complex **1** (1 mM, panel A), complex **2** (1 mM, panel B), and C) complex **3** (1 mM, panel in H_2O/CH_3CN (1:4) / NBu_4PF_6 0.1 M under argon (black curve) and CO_2 (saturated, blue curve). Orange curve: CV of a CO_2-saturated solution without Ni complex.

4.2. CV of complexes 1 in CH_3CN/H_2O (4:1) under Ar at different scan rates

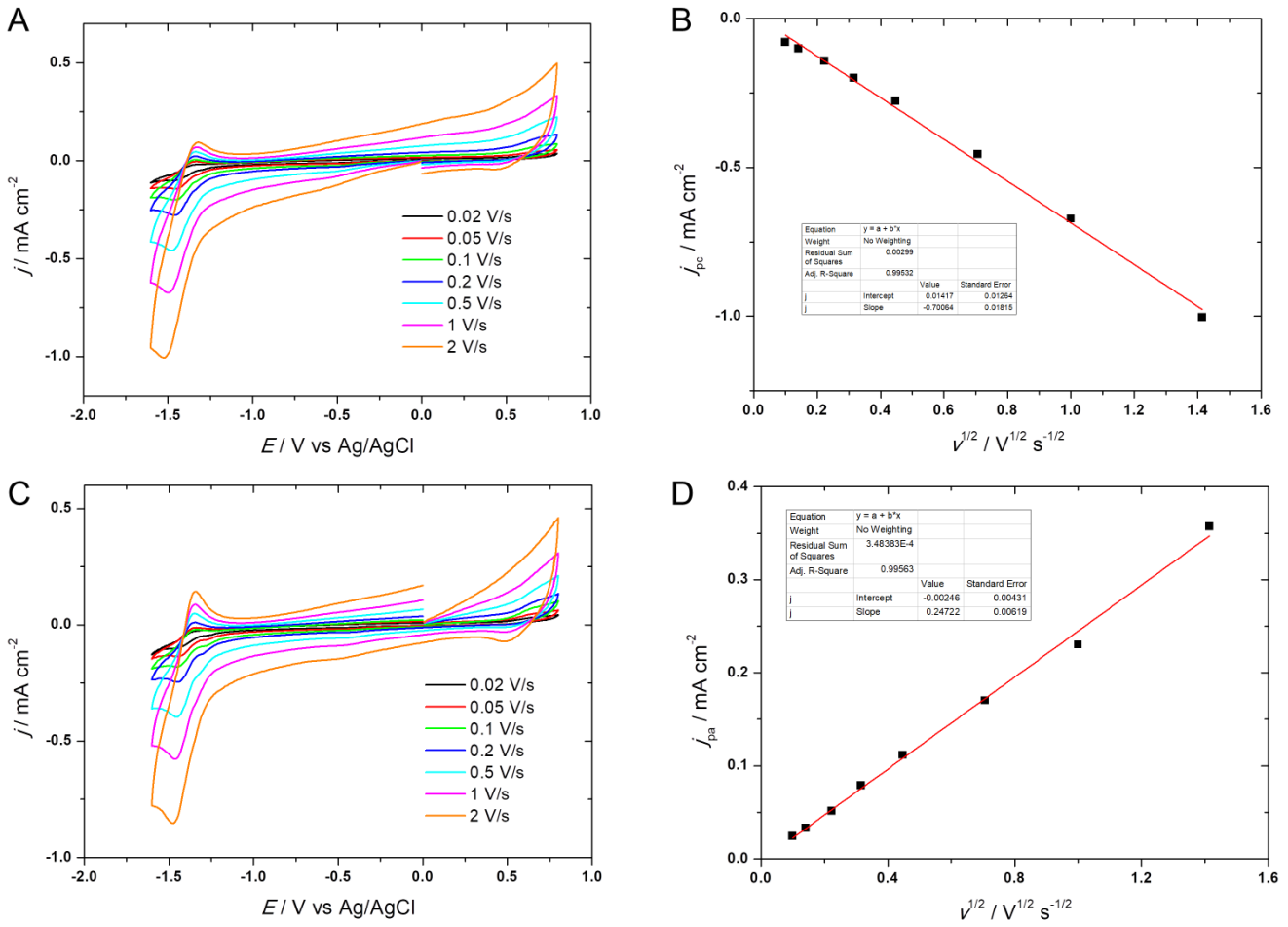

Figure S17. A) and C) CVs at different scan rates (0.02 $V.s^{-1} < v < 2\ V.s^{-1}$) at a glassy carbon working electrode of complex **1** (1 mM) in H_2O/CH_3CN (1:4) / NBu_4PF_6 0.1 M under argon, for negative (panel A) and positive (panel C) scanning direction; B) and D) Plots of peak current densities against $v^{1/2}$ ($0.01\ V.s^{-1} < v < 2\ V.s^{-1}$) for the $Ni^{II/I}$ (j_{pc}, panel B) and $Ni^{III/II}$ (j_{pa}, panel D) redox systems.

5. XPS surface and voltammetric characterization of Au-1 electrodes

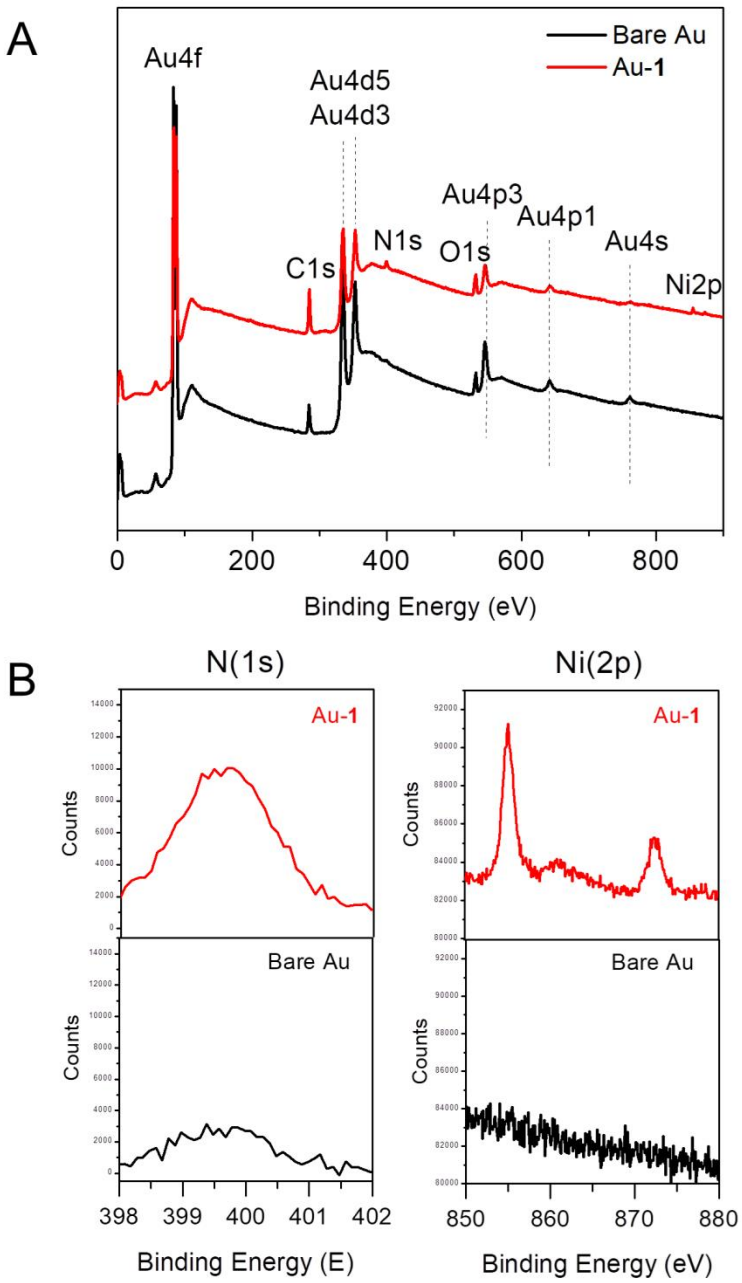

Figure S18. XPS spectra for the Au-**1** (red) and bare Au (black) wafers. A) Large energy range (0-900 eV); B) Restricted energy range for N(1s) and Ni(2p).

The fitted XPS spectra of C(1s) signals of bare and modified gold surfaces (Figure S19) display an increase of C-C bond percentage from 32 to 40 % at 285 eV and C-N type bond at 286 eV from 6 to 13 % (Table S1). This result is a further evidence of the presence of the Ni complex on the surface.

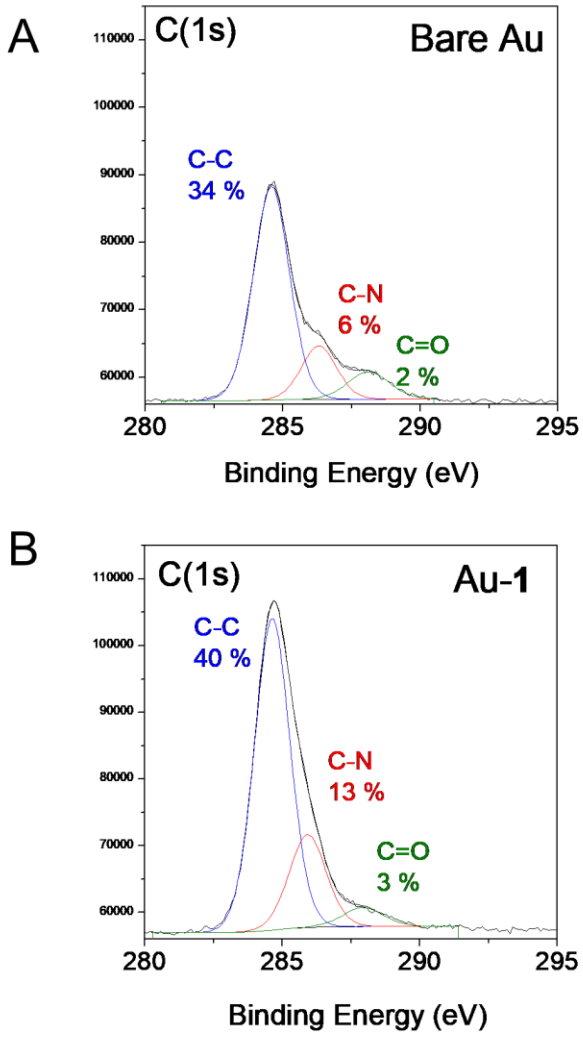

Figure S19. XPS C(1s) spectra of a bare gold surface (panel A) and a functionalized Au-**1** surface (panel B), including deconvolution into C-C, C-N and C=O contributions.

Table S1. Relative peak areas (in %) from the fitted C(1s) spectra of bare gold and Au-**1** surfaces from XPS analysis.

	C (1s)	C-C	C-N	C=O
Bare gold	42	34	6	2
Au-**1**	56	40	13	3

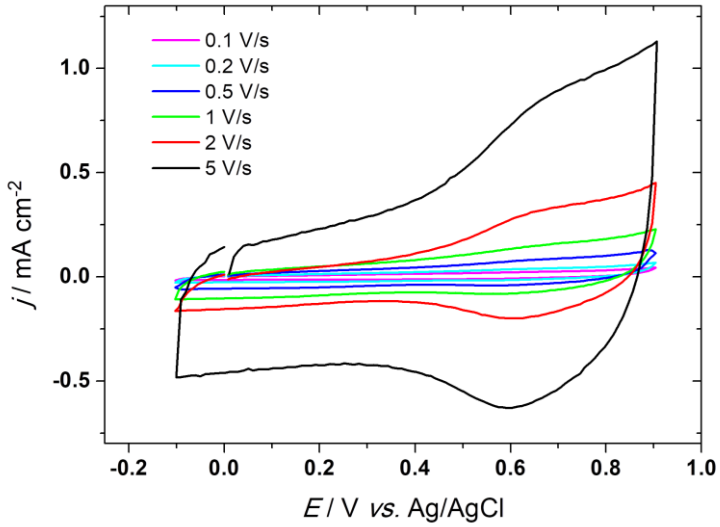

Figure S20. A) CVs of an Au-**1** modified electrode in H_2O/CH_3CN (1:4) / NBu_4PF_6 0.1 M under argon at different scan rates (0.1 $V.s^{-1} < v < 5\ V.s^{-1}$).

6. Voltammetric characterization of GC-1 electrodes

6.1 CVs of GC-1 under CO_2 and Ar

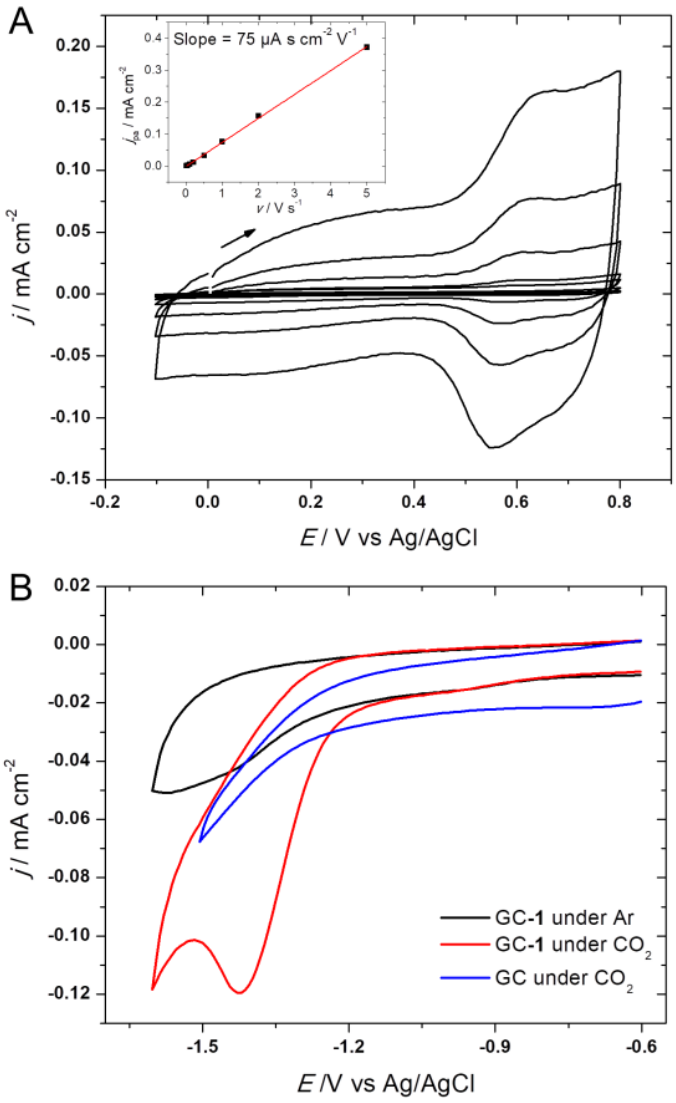

Figure S21. A) CVs of a GC-**1** modified electrode in H_2O/CH_3CN (1:4) / NBu_4PF_6 0.1 M under argon at different scan rates (0.02 $V.s^{-1} < v < 2$ $V.s^{-1}$). Inset: Plots of j_{pa} *vs.* *v*; B) CVs (v = 0.1 $V.s^{-1}$) of a GC-**1** electrode under argon (black curve) and CO_2 (saturated, red curve). For comparison, the blue curve displays the CV of an unmodified GC electrode under CO_2 (saturated).

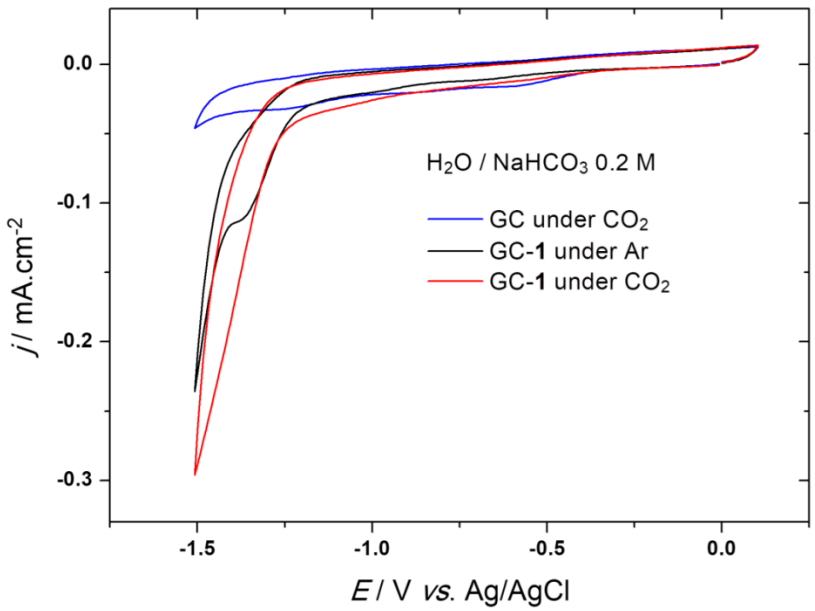

Figure S22. CVs (v = 0.1 V.s^{-1}) at a GC-**1** electrode under argon (black curve) and CO_2 (saturated, red curve) in H_2O / $NaHCO_3$ 0.2 M (pH = 6.8). For comparison, the blue curve displays the CV of an unmodified GC electrode under CO_2.

6.2 Determination of the electron transfer kinetics for GC-1

According to Laviron,[5] the increase of both anodic and cathodic peak potential values with scan rate (Figure S22-A), can be exploited to evaluate electron-transfer kinetics between the grafted species and the electrode, assuming that kinetics is not too fast ($k^0 < 10^3$ s^{-1}), and that redox centers are considered as non-interacting between each other. When $\Delta E_p/n < 200$ mV at high scan rate [ΔE_p is the peak-to-peak separation, and n the number of electrons exchanged (n=1)], the standard rate constant k^0 can be determined from the variation of $n\Delta E_p$ with v, according to the parameter m defined as given in equation S1:

$$m = \frac{RT}{nF}\frac{k^0}{v} \qquad \text{(Equation S1)}$$

In the specific case of GC-**1**, one can assume that the transfer coefficient α approximates 0.5 from the symmetrical variation of E_{pa} and E_{pc} with log v (Figure S22-A). The best match between the theoretical ΔE_p vs m^{-1} curve for α = 0.5 and the experimental data was obtained for k^0 = 33 +/- 3 s^{-1} (Figure S22-B).

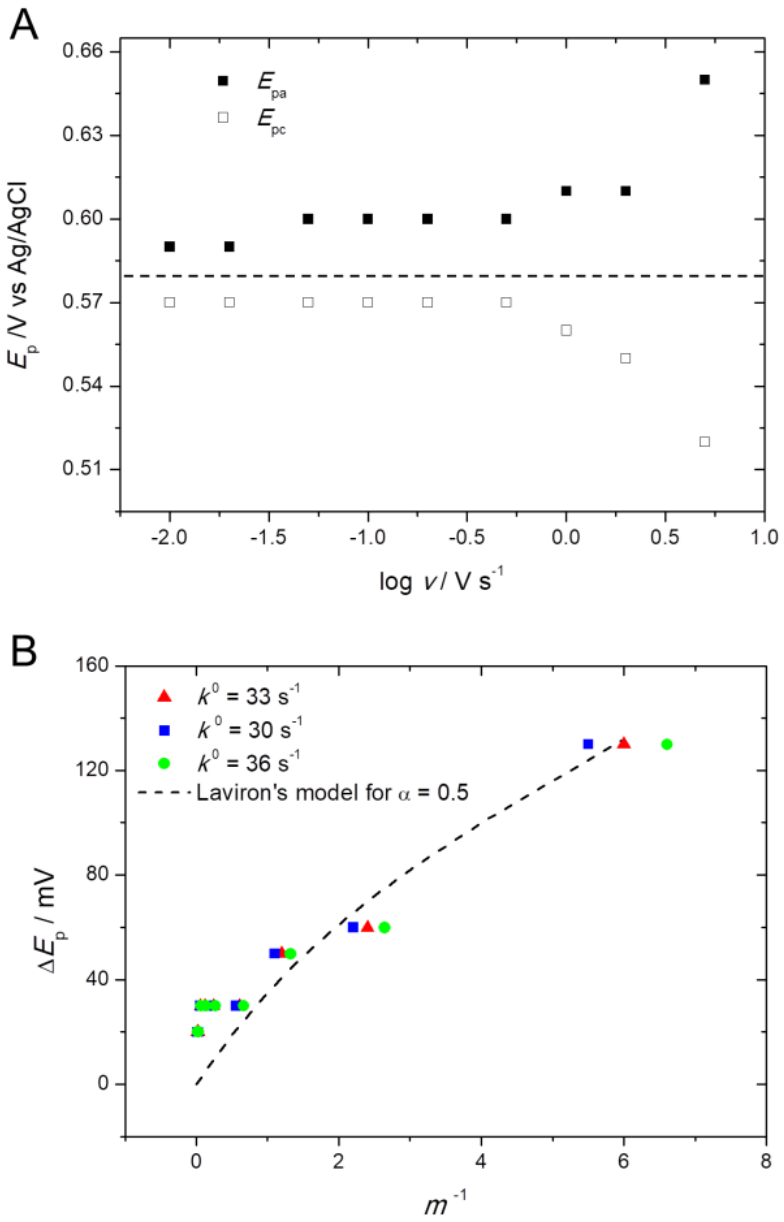

Figure S23. A) Plots of E_{pa} (black squares) and E_{pc} (white squares) *vs*. log *v* for measurements performed at different scan rates with a modified GC-**1** electrode in H_2O/CH_3CN (1:4) / NBu_4PF_6 0.1 M under argon [the dashed line represents the $E_{1/2}$ value at 0.58 V vs Ag/AgCl]; B) Plots of ΔE_p vs m^{-1} assuming three different values for the standard rate constant k^0 : 33 s^{-1} (red triangles), 30 s^{-1} (blue squares), 36 s^{-1} (green circles) [the dashed line corresponds to theoretical variation of ΔE_p vs m^{-1} calculated by Laviron assuming α = 0.5].

7. Voltammetric characterization of GC-CNT-1 and GC-CNT-3 electrodes

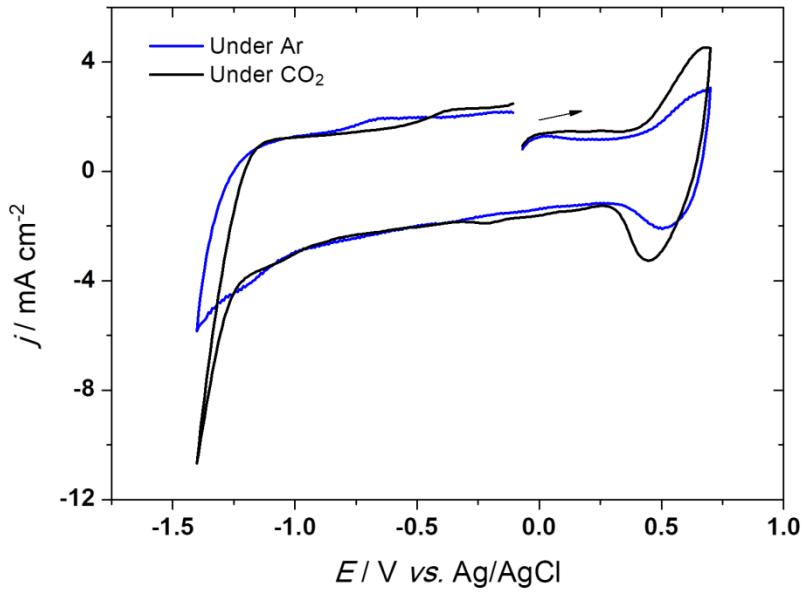

Figure S24. CVs (v = 0.1 V.s^{-1}) under Ar (blue) and under CO_2 (black) of GC-CNT-**1** electrodes in $LiClO_4/H_2O$ 0.1 M (pH=7.0).

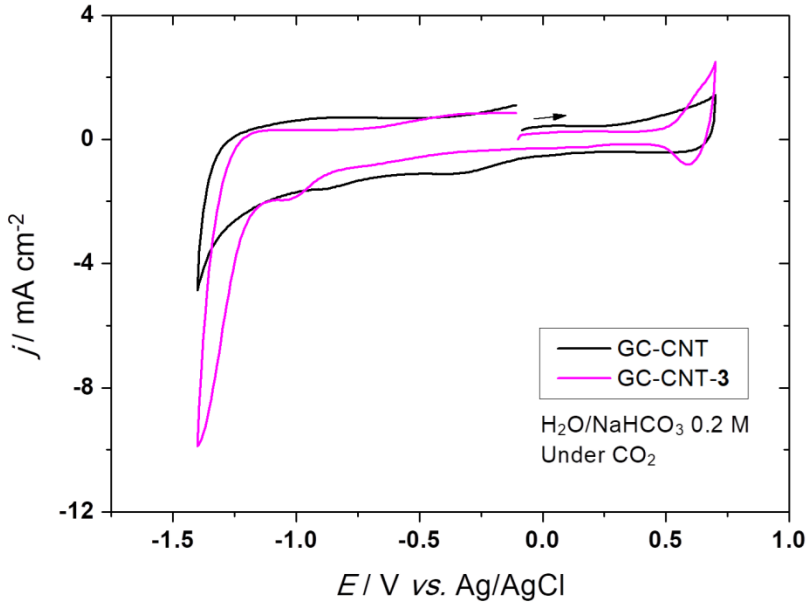

Figure S25. CVs (v = 0.1 V.s^{-1}) under CO_2 of GC-CNT (black) and GC-CNT-**3** (pink) electrodes in $LiClO_4/H_2O$ 0.1 M (pH=7.0).

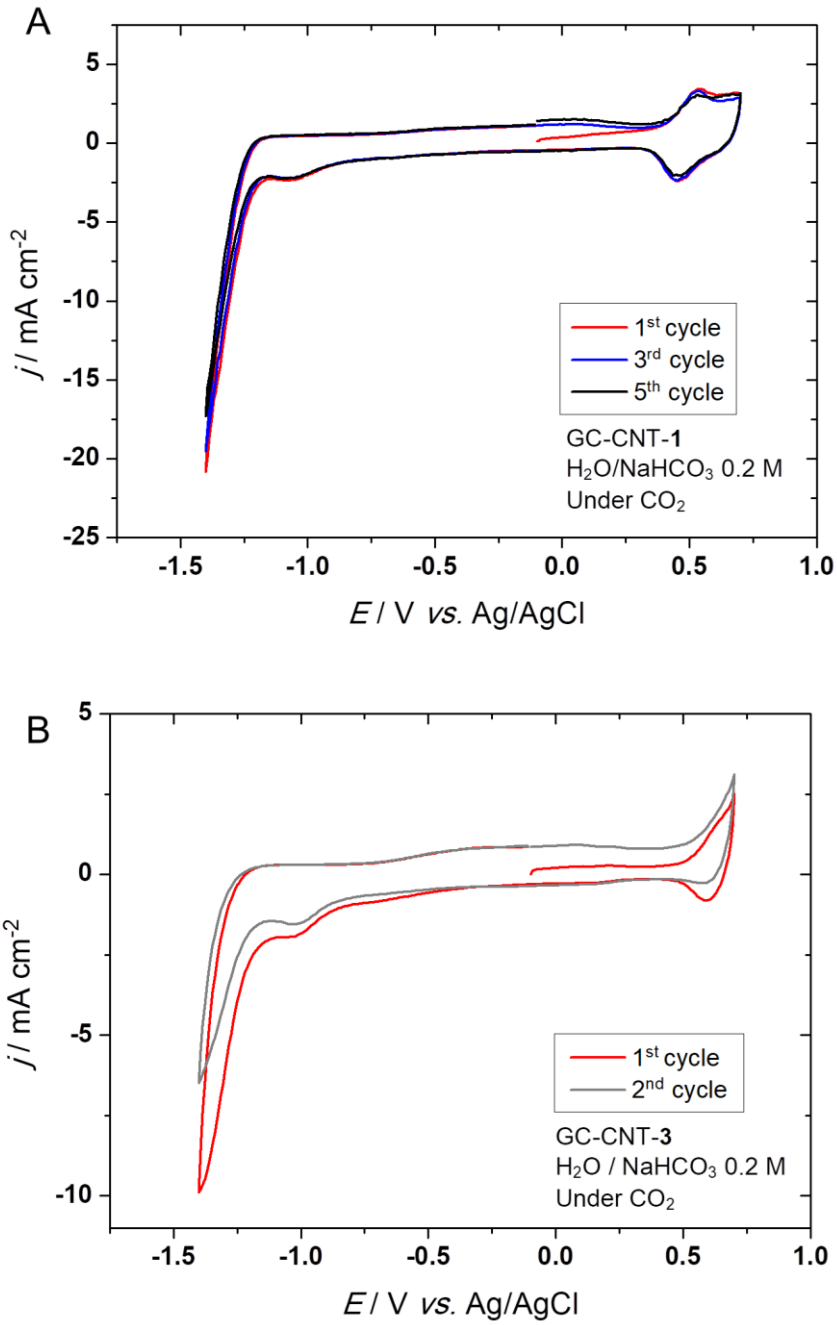

Figure S26. CVs (v = 0.1 V.s^{-1}) under CO_2 of A) GC-CNT-**1** and B) GC-CNT-**3** in $NaHCO_3/H_2O$ 0.2 M (pH=6.8).

8. Controlled-potential electrolysis with GC-CNT-1 electrodes

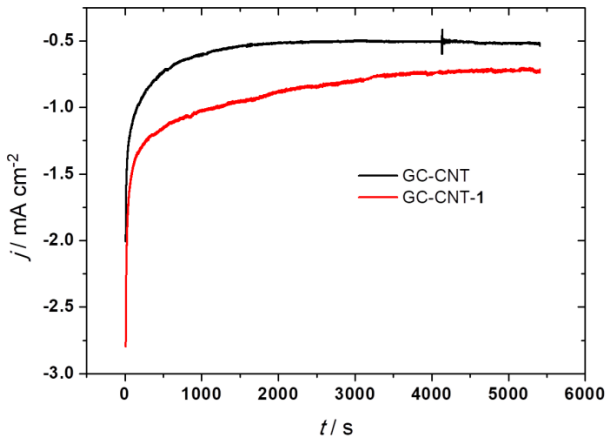

Figure S27. Plots of current density *vs*. time obtained during electrolysis of a CO_2-saturated solution of Na-HCO3/H_2O 0.2 M (E_{app} = -1.25 V *vs*. Ag/AgCl) with GC-CNT (black) and GC-CNT-**1** (red) electrodes.

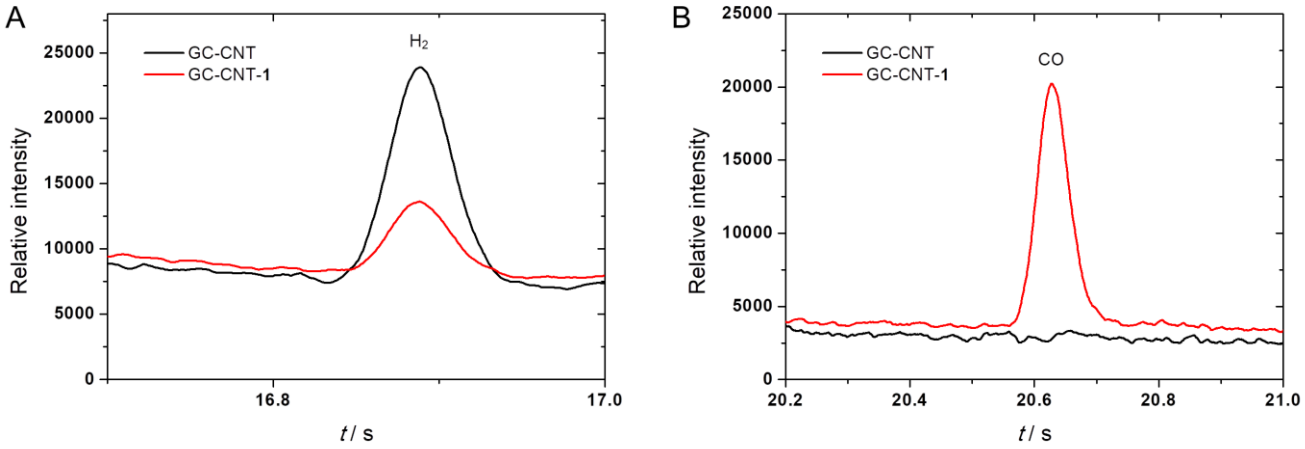

Figure S28. Gas chromatography analysis of the A) H_2 (t = 16.9 min) and B) CO content (t = 20.6 min) in the gaseous atmosphere obtained 1h30 electrolysis of a CO_2-saturated solution of H_2O/$NaHCO_3$ 0.2 M by using GC-CNT (black) and GC-CNT-**1** (red) working electrodes (E_{app} = -1.25 V vs. Ag/AgCl).

Table S2. Gas chromatography analysis data for CO and H_2 obtained 1h30 electrolysis at E_{app} = -1.25 V *vs*. Ag/AgCl in a CO_2-saturated solution of $NaHCO_3$/H_2O 0.2 M by using either a GC-CNT-**1,** GC-CNT-**3**, or GC-CNT working electrode.

Electrode	***n* (CO) nmol**	**TON CO**	**FY %**	***n* (H_2) nmol**	**FY %**
GC-CNT-**1**	590	454	56	110	11
GC-CNT-**3**	47	310	12	116	29
GC-CNT	-	-	-	790	35

Additional information for gas chromatography experiments

Injection Mode: Split
Temperature: 200.0 C
Carrier Gas: He
Flow Control Mode: Velocity
Pressure: 219.7 kPa
Total Flow: 176.5 mL/min
Column Flow: 3.40 mL/min
Linear Velocity: 40.0 cm/sec
Purge Flow: 3.0 mL/min
Split Ratio: 50.0
High Pressure Injection: Off
Carrier Gas Saver: On
Split Ratio: 10.0
Time: 0.80 min
Splitter Hold: Off

Column oven
Initial Temperature: 35.0 C
Equilibration Time: 1.0 min
Temperature Program:

	Rate (°C/min)	Temperature (°C)	Hold Time (min)
1	50.00	160.0	3.50
2	-50.00	40.0	4.50
3	20.00	60.	4.00

Column Information
Column Name: MS5A and PPQ
Film Thickness: 18.00 um
Column Length: 60.0 m
Inner Diameter: 0.32 mm ID
Column Max Temp: 250.0 °C
Cooling Speed Switching Temp.: 200.0
Cooling Speed: High

Detector 1 BID1
Temperature: 200.0 C
Sampling Rate: 40 msec
Stop Time: 21.90 min
Subtract Detector: None
Discharge Gas: He
Discharge Gas Flow: 50.0 mL/min

9. References

1 N. Camus, Z. Halime, N. Le Bris, H. Bernard, C. Platas-Iglesias and R. Tripier, *J. Org. Chem.*, 2014, **79**, 1885-1899.

2 Z. Halime, M. Frindel, N. Camus, P. Y. Orain, M. Lacombe, K. Bernardeau, M. Cherel, J. F. Gestin, A. Faivre-Chauvet and R. Tripier, *Org. Biomol. Chem.*, 2015, **13**, 11302-11314.

3 A. Filali, J.-J. Yaouanc and H. Handel, *Angew. Chem. Int. Ed.*, 1991, **30**, 560-561.

4 B. Bosnich, M. L. Tobe and G. A. Webb, *Inorg. Chem.*, 1965, **4**, 1109-1112.

5 E. Laviron, *J. Electroanal. Chem.*, 1979, **101**, 19-28.